Clim Dyn
DOI 10.1007/s00382-009-0667-8

Understanding the West African monsoon variability and its remote effects: an illustration of the grid point nudging methodology

Soline Bielli · Hervé Douville · Benjamin Pohl

Received: 19 December 2008 / Accepted: 8 September 2009

Abstract General circulation models still show deficiencies in simulating the basic features of the West African Monsoon at intraseasonal, seasonal and interannual timescales. It is however, difficult to disentangle the remote versus regional factors that contribute to such deficiencies, and to diagnose their possible consequences for the simulation of the global atmospheric variability. The aim of the present study is to address these questions using the so-called grid point nudging technique, where prognostic atmospheric fields are relaxed either inside or outside the West African Monsoon region toward the ERA40 reanalysis. This regional or quasi-global nudging is tested in ensembles of boreal summer simulations. The impact is evaluated first on the model climatology, then on intraseasonal timescales with an emphasis on North Atlantic/Europe weather regimes, and finally on interannual timescales. Results show that systematic biases in the model climatology over West Africa are mostly of regional origin and have a limited impact outside the domain. A clear impact is found however on the eddy component of the extratropical circulation, in particular over the North Atlantic/European sector. At intraseasonal timescale, the main regional biases also resist to the quasi-global nudging though their magnitude is reduced. Conversely, nudging the model over West Africa exerts a strong impact on the frequency of the two North Atlantic weather regimes that favor the occurrence of heat waves over Europe. Significant impacts are also found at interannual timescale. Not surprisingly, the quasi-global nudging allows the model to capture the variability of large-scale dynamical monsoon indices, but exerts a weaker control on rainfall variability suggesting the additional contribution of regional processes. Conversely, nudging the model toward West Africa suppresses the spurious ENSO teleconnection that is simulated over Europe in the control experiment, thereby emphasizing the relevance of a realistic West African monsoon simulation for seasonal prediction in the extratropics. Further experiments will be devoted to case studies aiming at a better understanding of regional processes governing the monsoon variability and of the possible monsoon teleconnections, especially over Europe.

This paper is a contribution to the special issue on West African Climate, consisting of papers from the African Multidisciplinary Monsoon Analysis (AMMA) and West African Monsoon Modeling and Evaluation (WAMME) projects, and coordinated by Y. Xue and P. M. Ruti.

S. Bielli (✉) · H. Douville · B. Pohl
CNRM/GMGEC/UDC, Météo-France, 42 avenue Coriolis, 31057 Toulouse Cedex 01, France
e-mail: soline.bielli@cnrm.meteo.fr

1 Introduction

The West African monsoon (WAM) provides most of the rainfall for West African countries. Embedded in the radiatively forced seasonal migration of the inter-tropical convergence zone (ITCZ), it shows a strong annual cycle but also a strong variability on a wide range of scales. The intraseasonal and interannual fluctuations of the WAM are relatively well documented and have been the focus of considerable research. Superimposed on lower frequency fluctuations, dry spells within the monsoon season and/or dry years can have devastating environmental and socio-economical impacts, especially in the Sahel where food production is highly dependent on rain-fed crops. Thus, predicting the rainfall season and its sub-seasonal distribution is crucial for farmers and aid planning.

Published online: 22 September 2009

Unfortunately, there are still fundamental gaps in our knowledge of the WAM variability. This is partly due to the lack of appropriate observational datasets and it is the reason why the African monsoon multidisciplinary analysis (AMMA) project has been launched in 2003 (Redelsperger et al. 2006). It is both an international research program and a multi-year field campaign whose ultimate goal is to understand how scale and process combinations shape the mean monsoon and its variability. While most emphasis is on the interaction between the convective to synoptic scale and the regional scale, less attention has been paid to the interaction between the regional scale and the global scale.

Yet, both observational and numerical studies have suggested strong relationships between the WAM and other tropical or extratropical areas. On interannual timescales, the sensitivity of the WAM to remote sea surface temperature (SST) anomalies such as the El Niño Southern Oscillation (ENSO) in the equatorial Pacific has been well documented (i.e. Janicot et al. 2001; Rowell 2001). On intraseasonal timescales, the modulation of the WAM by the Indian summer monsoon (Rodwell and Hoskins 1996) and the Madden–Julian/Intraseasonal Oscillation (Matthews 2004; Janicot et al. 2009; Pohl et al. 2009) has also been suggested. Conversely, the WAM is supposed to play a significant role in the global energy budget and in the global atmospheric circulation (Webster et al. 1998). Mediterranean basin and Europe are obviously privileged targets for looking at the remote effects of the monsoon variability. Former observational studies (e.g. Raicich et al. 2003) indeed suggest possible relationships between the WAM and the Mediterranean climate at interannual timescale. Moreover, diagnostics both based on reanalyses and numerical sensitivity experiments (e.g. Cassou et al. 2005) show that anomalous diabatic heating related to monsoon rainfall variability over the Sahel could contribute to the occurrence of extreme weather events over Europe, such as the summer 2003 heatwave.

In the framework of AMMA, coordinated global atmospheric simulations driven by idealized SST anomalies have been performed to improve our understanding of the role of oceanic boundary conditions (Mohino Harris et al. 2008). While such experiments are useful to complete the more traditional AMIP-type experiments in which the models are driven by monthly mean observed SSTs (e.g. Moron et al. 2004), they are based on atmospheric general circulation models (GCM) that still show serious deficiencies in simulating the basic features of the WAM (e.g. Sperber and Palmer 1996; Moron et al. 2004). Such deficiencies are even more obvious in coupled ocean–atmosphere GCMs given their difficulties in simulating the tropical SSTs and their gradients, especially in the equatorial Atlantic Ocean. Most CMIP3 models do not place the summer precipitation maximum over the African continent, but over the warmly biased Gulf of Guinea (Cook and Vizy 2006). Most of them also fail in reproducing the high-frequency variance over the West African domain (Ruti and Dell' Aquila 2008) or the WAM seasonal teleconnections with the tropical oceans (Joly et al. 2007).

As a result, state-of-the-art coupled GCMs still show a limited skill in predicting West African rainfall anomalies at the intraseasonal to seasonal timescales (i.e. Garric et al. 2002) and a large spread in projecting the monsoon rainfall at the end of the 21st century (Douville et al. 2006). Such failures emphasize the need of process-oriented studies promoted by the AMMA project, but also the need of new numerical tools for understanding the complex scale interactions that control the WAM and its variability. On the one hand, it is almost impossible to disentangle the relative influence of remote versus regional forcings of the WAM using only observational datasets. On the other hand, the current-generation GCMs are not necessarily appropriate to design meaningful sensitivity experiments.

The IRCAAM project funded by the French National Research Agency and coordinated by CNRM (Centre National de Recherches Météorologiques, Météo-France, Toulouse) is an attempt to overcome such a problem by merging observations and atmospheric modeling in an original framework. The basic idea is to use the ERA40 reanalysis (Uppala et al. 2005) for guiding the CNRM atmospheric GCM over a prescribed domain. Such a technique allows us to constrain a realistic model trajectory within the domain in order to analyze the consequences for the model trajectory outside of the domain. The ultimate objective of IRCAAM is to explore the physical and dynamical mechanisms that underlie the intraseasonal and interannual variability of the summer monsoon climates, their reciprocal influence, and their remote effects on the extratropics.

The present study is both an extension and an illustration of the IRCAAM strategy applied in the framework of AMMA. It is based on global atmospheric simulations driven by prescribed monthly mean SST in which the Arpege-Climat model is guided toward ERA40 either outside or within the WAM domain. The objective is twofold. First, explore to what extent a "perfect" simulation outside of the WAM domain (quasi-global nudging) would improve the simulation of the monsoon. Secondly and conversely, explore to what extent a "perfect" simulation of the WAM (African nudging) would improve the simulation of the global atmospheric circulation. Here by "perfect" we mean as good as the 6-hourly ERA40 reanalysis are compared to the real atmosphere.

Note that the spectral nudging technique has been widely used in the regional climate modeling community for avoiding a drift in the large-scale circulation (e.g. Von Storch et al. 2000). Here, the approach is different: it is

based on a grid point nudging methodology applied over a limited domain and the objective is to evaluate the consequences outside rather than inside the nudging domain (e.g. Jung et al. 2008). The experimental design is detailed in Sect. 2. The results are described in Sect. 3 to 5 by distinguishing the nudging impacts on mean climate, intraseasonal variability and interannual variability respectively. Conclusions and prospects are given in Sect. 6.

2 Model and experimental design

All simulations are based on version 4 of the Arpege-Climat model derived from the Arpege/IFS numerical weather prediction model developed jointly by the European Centre for Medium-range Weather Forecasts (ECMWF) and Météo-France. It is a spectral model with a progressive hybrid σ-pressure vertical coordinate. The model is used in its standard configuration (linear T63 truncation, reduced 128 by 64 Gaussian grid, 31 vertical levels). The dynamical core is close to the one used at ECMWF with a semi-implicit, semi-Lagrangian, two-time level discretization scheme. The physical package is partly inherited from the Météo-France operational weather forecast model and it is very similar to the one used by CNRM in the CMIP3 simulations (Salas y Mélia et al. 2005). In particular, it includes a mass flux convective scheme with a Kuo-type closure (Bougeault 1985) that has a strong impact on the vertical profile of diabatic heating in the tropical troposphere.

The regional nudging is applied at each time step to the horizontal wind components (u and v), temperature (T), specific humidity (q) and mean sea-level pressure (MSLP) in order to exert a strong control on the tropical atmosphere. Sensitivity experiments were performed where temperature and/or specific humidity were not nudged. Results showed that the monsoon precipitation was better constrained when nudging both temperature and specific humidity in addition to the wind components.

The nudging is implemented by adding an extra term to the model prognostic equations. This term takes the form $-\lambda(y - y_{\text{ref}})$ where y is the state of the model, y_{ref} is the reference field toward which the model is relaxed and $\lambda = t_{\text{step}}/e_{\text{time}}$ is the strength of the relaxation with t_{step} the time step of integration (30 min) and e_{time} the e-folding relaxation time. The strength of the relaxation λ is varied according to the variable (5-h e-folding time i.e. $\lambda = 0.1$ for u and v, and 12 h e-folding time i.e. $\lambda = 0.04$ for the other variables) and the vertical level (weaker at the 3 lowest and 5 highest levels) to let the model adjust to the nudging. λ is taken uniform horizontally in the nudging domain. Although Arpege-Climat is a spectral atmospheric model, here the nudging is achieved on a limited 3D domain and therefore on the Gaussian grid after an inverse spectral transform.

The 6-hourly ECMWF re-analyses (ERA40) have been used as a reference to prescribe the tropical atmosphere in the nudged experiments. The control experiment, CtCl, is a 30-year simulation (after a 2-year spin-up) driven by the ERA40-monthly mean climatological SSTs averaged over the 1971–2000 period. A parallel 1971–2000 integration, CtIV, has been performed using the observed ERA40-monthly mean SSTs, including their interannual variability. Although both experiments show very similar climatologies, they will serve as alternative references for evaluating the impact of the nudging in comparison with the influence of the SST forcing. All nudged experiments consist in ensembles of 30 boreal summer integrations initialized on May 15th from each of the individual year of CtCl. Daily outputs have been archived from June 1st to September 30th (hereafter the JJAS season), i.e. after a 15-day spin-up allowing the Arpege-Climat model to adjust to the nudging and/or the SST perturbation.

Two domains of nudging have been considered (Fig. 1): West Africa (African nudging, AfNu experiments) and the remaining part of the global atmosphere (quasi-global nudging, NAfNu experiments). The AfNu domain is comprised between 10°S–28°N and 40°W–50°E. It is surrounded by a 5° buffer zone in which the nudging vanishes progressively in order to ensure a smooth transition between the nudged and free atmosphere. For the quasi-global nudging experiments, the nudging is applied outside the following region: 10°S–32°N and 30°W–50°E (Fig. 1). The two experiments are therefore not perfectly symmetric. This is because they were not designed to be compared to each other, but rather to a common control experiment without nudging. Moreover, the main objective of the AfNu experiment is to explore the impact on the simulation of the European climate, so that the northern boundary of the nudging domain should be located southwards of 30°N given the presence of a 5° buffer zone between the relaxed and free atmosphere.

The basic set of experiments is summarized in Table 1. For each domain of nudging, the impact of the atmospheric nudging is assessed using either observed (monthly mean) or climatological monthly SST. Such a strategy is useful not only to assess the robustness of the nudging impacts, but also to explore the possible interaction between the atmospheric relaxation and the SST forcing outside the domain of nudging. While this issue will be mainly highlighted in the analysis of interannual variability, here the focus is mostly on mean climate and intraseasonal variability. For this reason, the model is not nudged toward a particular year of ERA40, but successively toward each boreal summer season comprised between 1971 and 2000. These experiments will first be used to address the

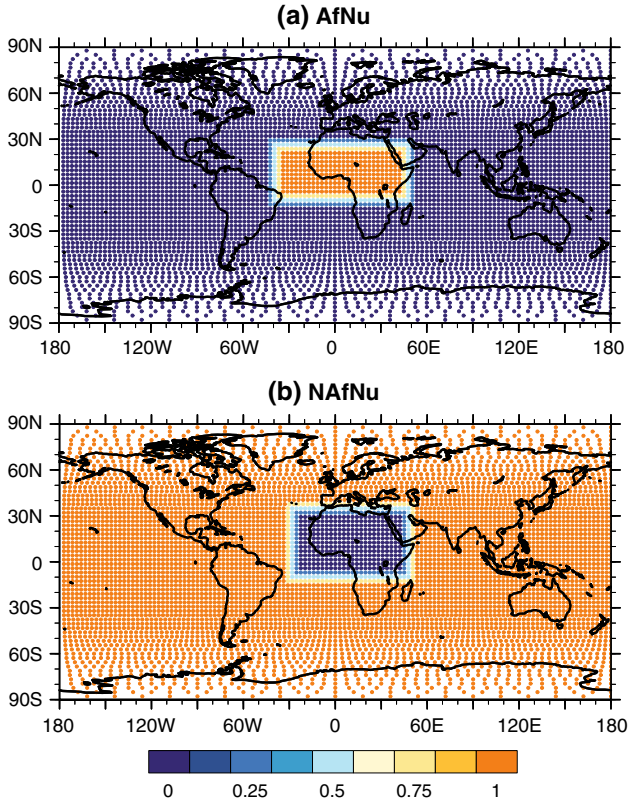

Fig. 1 The two masks used for implementing the nudging toward ERA40 in the Arpege-Climat model, with a smooth transition between full (1) and no (0) nudging. **a** Mask for the nudging inside West Africa (AfNu) and **b** Mask for the nudging outside West Africa (NAfNu)

following questions. What are the regional versus remote contributions to the model systematic biases over West Africa? Conversely, what would be the benefit of a perfect simulation of the WAM for the global climatology of the Arpege-Climat atmospheric GCM?

3 Mean climate

3.1 JJAS latitude-pressure cross section above West Africa

Figure 2 shows vertical cross section of the seasonal mean zonal wind and temperature for CtIV along with the model biases for all experiments averaged between 15°W and 15°E and from 1971 to 2000. The Arpege-Climat model is able to reproduce the three dominant features of the atmospheric circulation over West Africa: the Tropical Easterly Jet (TEJ) at 200 hPa, the African Easterly Jet (AEJ) at 600 hPa and the westerly component of the low-level monsoon flow, but with important biases (Fig. 2a, b). Compared to ERA40, the control simulation (Fig. 2a, b) fails in simulating the intensity of the TEJ, AEJ and monsoon flow. The AEJ position is too low and it is shifted southward in the CtIV experiment. The latitudinal extent of the westerly component of the monsoon flow is smaller in CtIV with a reduction of the wind toward the south. The model is also too warm in the mid-troposphere and too cold in the upper troposphere. Very similar biases are found in the experiment using climatological SSTs (CtCl).

In the quasi-global nudging experiment (NAfNu, Fig. 2c, d), the warm bias around 600 hPa inside the WAM domain is significantly reduced, as well as the cold bias above 300 hPa. For the zonal wind, the impact is mainly found in the mid-troposphere, even if the AEJ is still shifted toward the equator compared to ERA40. The improvement is less clear in the lower and upper levels. This is partly due to the reduced intensity of the nudging strength at the top and bottom of the model.

In the AfNu experiment (AfNu, Fig. 2e, f), the temperature and zonal wind cross section is, less surprisingly, not significantly improved outside the domain. The warm and cold biases respectively around 600 hPa and aloft are reduced, but the wind biases resist between 15°W and 15°E, which is also true when looking at the zonal mean circulation over the whole extratropics (not shown).

3.2 JJAS low-level circulation and precipitation

Figure 3 presents the mean 925-hPa horizontal wind and precipitation fields during the JJAS season, as well as the model biases for all experiments. The most important bias of the control run (Fig. 3b) is a too weak low-level monsoon flow, particularly pronounced in the zonal component of the wind over the equatorial Atlantic. Westerly biases occur over the northeastern Sahara, resulting in a weakened Harmattan. Consequently, rainfall amounts over West

Table 1 Summary of the 6 30-JJAS simulations performed with the Arpege-Climat model

Exp. name	CtCl	CtIV	AfNuCl	AfNuIV	NAfNuCl	NAfNuIV
SST	Clim	Obs	Clim	Obs	Clim	Obs
Nudging	No	No	Yes	Yes	Yes	Yes
Nudging domain			Inside (10°S:28°N; 40°W:50°E]		Outside [10°S:32°N; 30°W:50°E]	
Nudged variables			*u*, *v*, *T*, *q*, MSLP		*u*, *v*, *T*, *q*, MSLP	
Relaxation time			*u*, *v*: 5 h *T*, *q*, MSLP: 12 h		*u*, *v*: 5 h *T*, *q*, MSLP: 12 h	

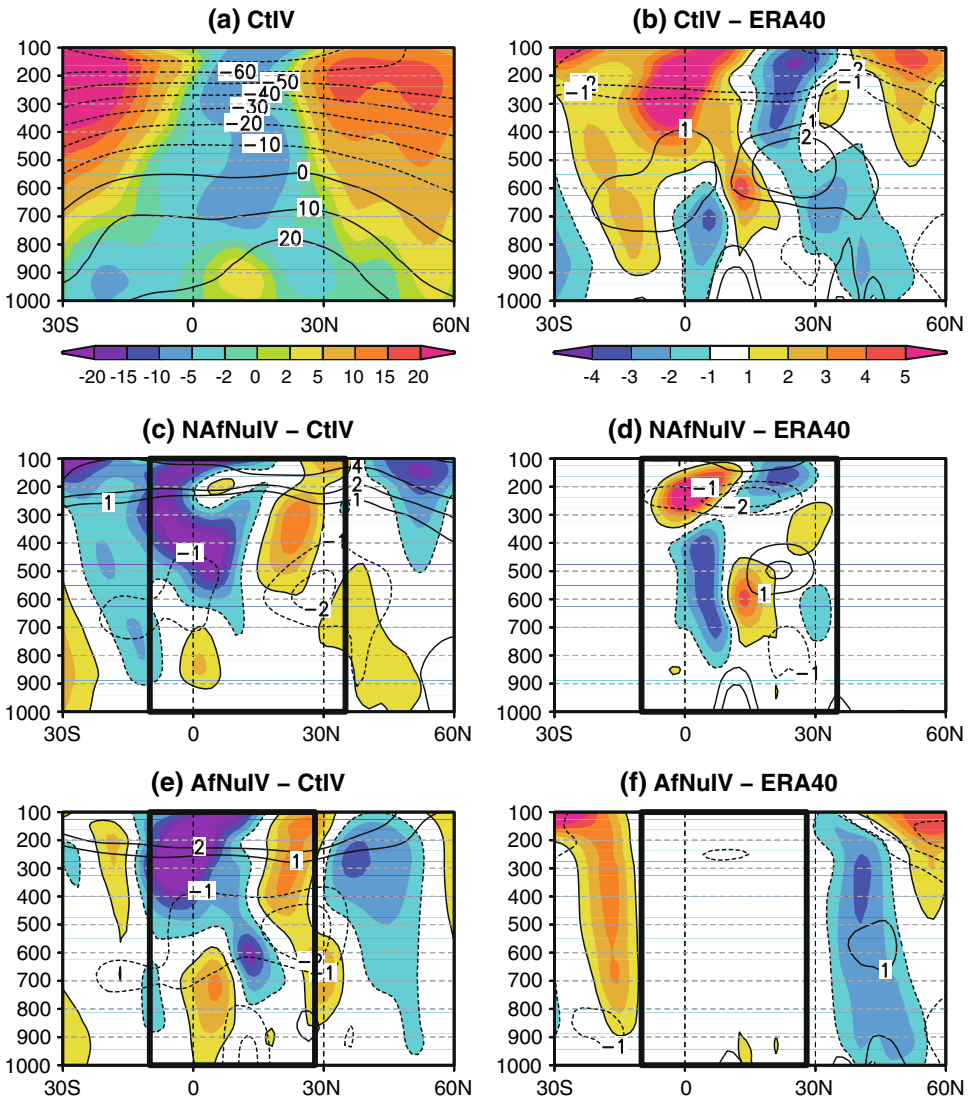

Fig. 2 Vertical cross section of JJAS zonal wind (m/s, *shaded*) and temperature (K, *contours*) averaged between 15°W and 15°E. *Left* and *right color bars* are for upper and other panel, respectively. In panel **c** to **f**, the domain of nudging is represented by a *black box*

Africa are also too low: the dryness in the model concerns the Congo basin, the Guinean belt and the Western Sahel. The Eastern Sahel and the East African Highlands are on the contrary too wet. Strong biases are also noted over the tropical oceans, where rainfall is far too abundant. Along the African coasts, the upwelling regions of the Benguela and the Canary islands constitute two major exceptions.

Although the monsoon flow is much more realistic, notably over the Atlantic Ocean, the Harmattan wind is still underestimated and the monsoon precipitation biases remain relatively strong (Fig. 3e, f). A RMS evaluation against ERA40 or GPCP and a comparison with CtlV (Fig. 3e) confirm the limited improvement in the precipitation climatology compared to the improvement of the monsoon circulation even in the lowest model levels. According to the RMS statistics, the zonal wind is improved by 50% (RMS reduction from 1.2 to 0.6) while the precipitation and meridional wind are only improved by about 35% (RMS reduction 1.83 to 1.19 and 1.34 to 0.85, respectively). This result shows the limits of the nudging technique, which is however here used to evaluate the consequences outside rather than inside the domain. Even though precipitation is improved, some biases persist in the AfNu experiment (Fig. 3e, f), thereby suggesting that tropical convection is only partly constrained by the large-scale circulation and the temperature and humidity profiles in the Arpege-Climat model.

In this respect, the biases of the control experiment are only partly improved in the NAfNu experiment (Fig. 3c, d). Over Africa, they present a very similar large-scale distribution than in CtlV (Fig. 3b). The RMS statistics however indicate noticeable improvements in the low-level zonal winds, particularly over the oceanic part of the domain (Fig. 3c). In AfNu, even though precipitation is still too strong (weak) in the eastern (western) part of the WAM region, nudging the regional circulation improves

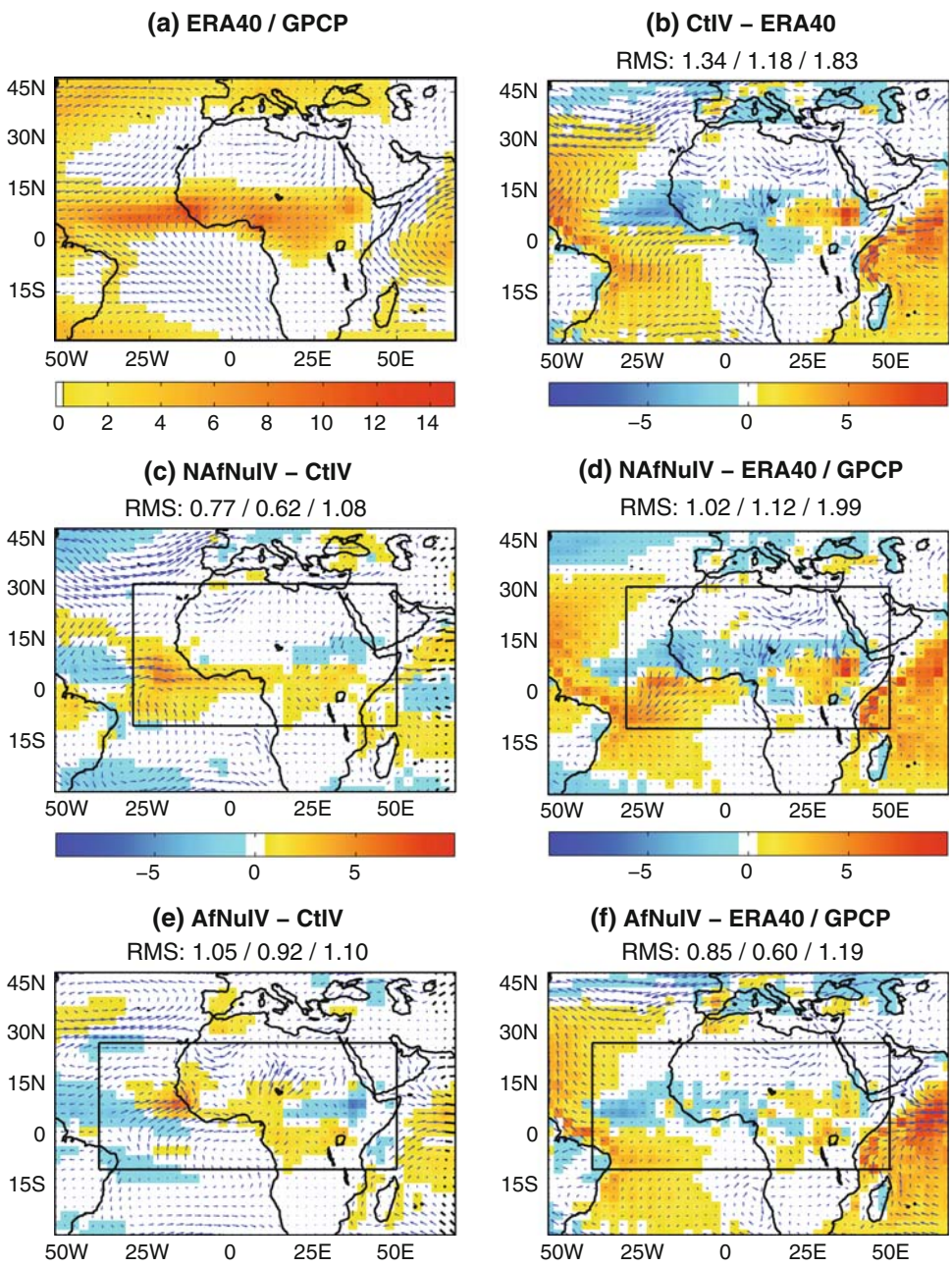

Fig. 3 **a** JJAS distribution of ERA40 925 hPa horizontal wind (m/s, *vectors*) and GPCP precipitation (mm/day, *shaded*). **b** Biases of CtlV experiment on the 1971–2000 period. Only the precipitation (wind) differences that are significant at the 95% confidence level according to a two-tailed Student (Hotelling) test are shown. The three RMS values are respectively for zonal wind, meridional wind and precipitation. **c** Differences between NAfNUIV and CtlV. **d** As **c** but for the biases of NAfNUIV. **e**, **f** As **c** and **d** but for AfNUIV

the representation of the three local maxima of precipitation (one centered on the West Coast near 8°N, the second near the mountains of Cameroon and the third over the mountains of Ethiopia, Hastenrath 1994). The first two are too weak and the third is too strong both in the control and in the NAfNu experiments. Note again that the nudging is weaker at 925 hPa than in the mid-troposphere, explaining partly the remaining biases in AfNu experiment.

Figure 4 shows the JJAS mean meridional wind at 200 hPa for ERA40 as well as the biases for all experiments. Again, the model biases are not reduced inside the WAM region when nudging outside the region (NafNu, Fig. 4c, d), confirming the regional nature of the main biases found over West Africa. On the contrary, the biases outside the WAM domain in AfNu are reduced, as shown by the strong negative correlation with the model biases and the close resemblance with the difference between NAfNu and the control experiment. Nudging the model over West Africa therefore seems to improve the simulation of the upper-troposphere stationary waves in the extratropics. This improvement is more striking in the southern hemisphere and is probably related to the propagation of Rossby waves and their interaction with the extratropical jets that are stronger in the winter than in the summer hemisphere (Hoskins and Ambrizzi 1993).

To sum up, on the one hand, the biases noted in the atmospheric circulation (Figs. 2, 3) and in the rainfall field (Fig. 3) tend to suggest that they are mostly of regional scale rather than the consequence of remote effects. On the other hand, while the impact of the nudging on the mean climate outside the nudging region is not major, some improvements are found both in the tropics and the extra-tropics (Fig. 2, 4). It is also important to note that there is no major discontinuity near the edge of the domain of nudging in any fields we have looked at, thereby suggesting that the transition from full nudging to no nudging is done smoothly enough and that the model responds physically to this relaxation technique.

3.3 Impact on northern hemisphere stationary waves in AfNu

In line with the impacts found in the upper troposphere circulation (Fig. 4), the impact of the nudging is more obvious when removing out the zonal mean response. Figure 5 shows the eddy component of the 500-hPa geopotential height (Z500) for ERA40, CtIV, differences between AfNuIV and CtIV and model biases with respect to ERA40. The biases of the control experiment correspond to both a lack of amplitude and a shift of the summer stationary waves over North Atlantic and Europe. Figure 5 indicates that nudging the model toward ERA40 over West Africa does not lead to a clear improvement of the JJAS stationary wave climatology over North Atlantic and Europe. Some features are improved, but the RMS over the whole North Atlantic/Europe sector is increased. This result does not mean that model deficiencies over West Africa are not relevant for simulating the summer climate over Europe, but that they are not the main source of errors in the Tropics. This hypothesis is confirmed by additional experiments (not shown) in which the nudging is applied over the whole tropical belt and where the impact on the mid-latitude stationary waves is clearly an improvement of the model climatology.

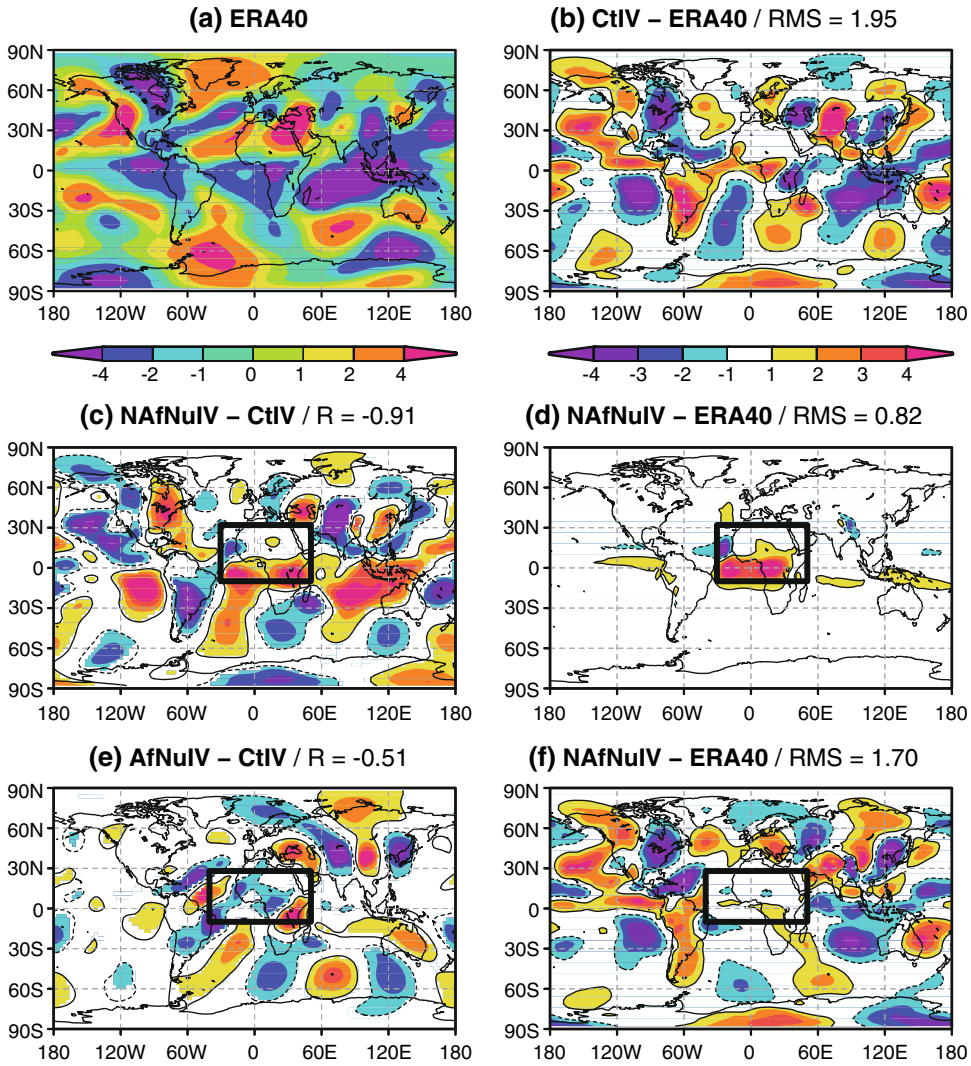

Fig. 4 Global distribution of JJAS meridional wind (m/s) at 200 hPa. *Left* and *right color bars* are for upper left and other panels, respectively. In panels **c** to **f**, the domain of nudging is represented by a *black box*. R in **c** and **e** denotes the correlation coefficient with **b**. RMS in **b**, **d** and **f** is the root mean square error against ERA40. Only differences being significant at the 95% confidence level according to a Student test are shown

4 Intraseasonal variability

4.1 West African intraseasonal variability

The day-to-day convective variability of the WAM is now investigated, with emphasis on the high frequencies within each JJAS season. The daily outgoing longwave radiation (OLR) fields are used as a proxy for atmospheric convection: here we compare the model outputs for AfNu, NAfNu and CtIV experiments with the ERA40 reanalyses. For each summer season, we first compute the standard deviation of the unfiltered daily OLR field, which is then averaged at each grid point over the 1971–2000 period. The resulting maps are shown in Fig. 6. The largest standard deviation values unambiguously correspond to the location of the ITCZ (Fig. 6a). Over Africa and the nearby Atlantic Ocean, they are confined between 5°N and 15°N.

Compared to the reanalyses, CtIV experiment shows important biases over the entire domain (Fig. 6b), denoting a too high intraseasonal variability in the OLR field. This is particularly true for the regions located on each side of the boreal summer ITCZ, i.e. between 15°N and 30°N and south of the equator. Additional analyses based on an OLR threshold of 220 W m^{-2}, used to distinguish deep convective clouds, reveal that convection remains active in the model ITCZ during approximately 95% of the days during JJAS. The model ITCZ also presents a latitudinal spread that is much larger than in the reanalyses or in the NOAAs' satellite observations. The intraseasonal variability in the model mostly concerns the number and extension of the convective events rather than their intensity. The overestimated latitudinal extent seems to be the main reason for the two zonal strips observed in Fig. 6b.

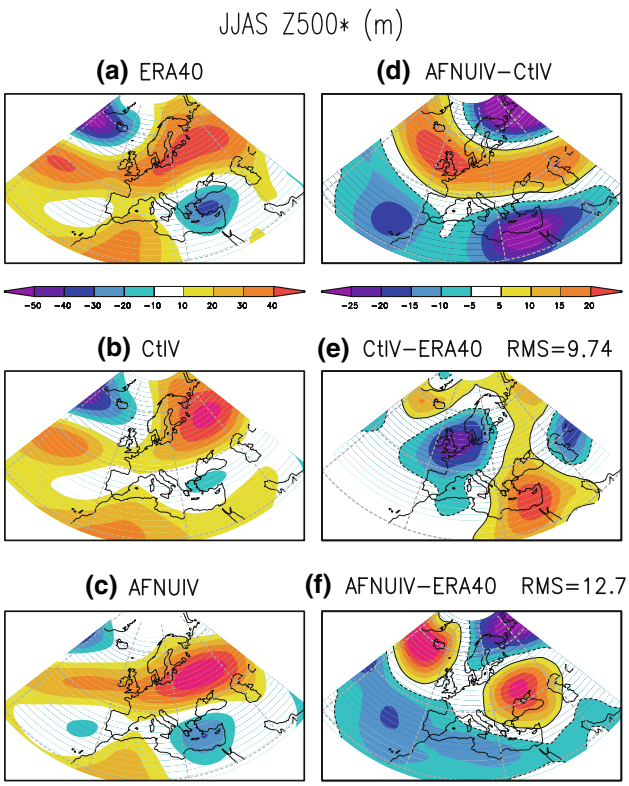

Fig. 5 JJAS distribution of the stationary-wave component of 500-hPa geopotential height (m) over North Atlantic and Europe. *Left* and *right color bars* are for left and right panels, respectively. **a** For ERA40. **b** For CtIV. **c** For AfNuIV. **d** Differences between AfNuIV and CtIV. **e** CtIV biases and **f** AfNuIV biases. In panels **e** and **f**, the RMS value is calculated over the region shown on this figure

The biases remain mostly unchanged over Africa in NAfNu experiment (Fig. 6d), showing again that they are mainly related to regional rather than remote factors. The standard deviation values abruptly increase over Africa, i.e. outside of the nudging window (Fig. 1). The nudging nonetheless reduces the biases over the non-nudging domain by 30% according to RMS statistics computed over the corresponding grid points for both CtIV and NAfNu experiments (Fig. 6b, d). Interestingly, similar zonal strips also appear over Africa in AfNu experiment, although their amplitude is dramatically decreased (with an RMS value reduced by more than 56% with respect to CtIV experiment).

In order to distinguish different ranges of the WAM intraseasonal variability in our different experiments, we next analyzed the standard deviation of the bandpass filtered OLR timeseries. Three intervals were retained: the 2–6-day range to document African easterly waves, and the 10–25-day and 25–60-day ranges identified as the dominant periodicities in the WAM by Sultan et al. (2003). Instead of showing the spatial patterns of the 2–6-day bandpass OLR fields, which is very close to that of the unfiltered data, we present the ratio between the standard deviation of filtered and unfiltered data (Fig. 7). Although not uniform, the latter generally varies between 40 and 50% compared to the unfiltered OLR series (Fig. 7).

The domain of preferred location for the easterly waves, extending from Central Africa toward West Africa, the equatorial Atlantic and the Caribbean islands, is well identified in the ERA40 reanalyses (Fig. 7a). In CtIV experiment this pattern is not so clear, and a too strong OLR variability is found over the Eastern Sahara, Arabia and the Western Arabian Sea. This bias is reduced in both AfNu and NAfNu experiments, providing a pattern of 2–6-day convective variance closer to the reanalyses.

Although not as clear, similar improvements apply for the 10–25 and the 25–60-day ranges, with standard deviations respectively decreased by 50 and 60% compared to the unfiltered OLR data. The areas concerned by the strongest convective activity remain the two zonal strips located north and south of the ITCZ, a feature strongly

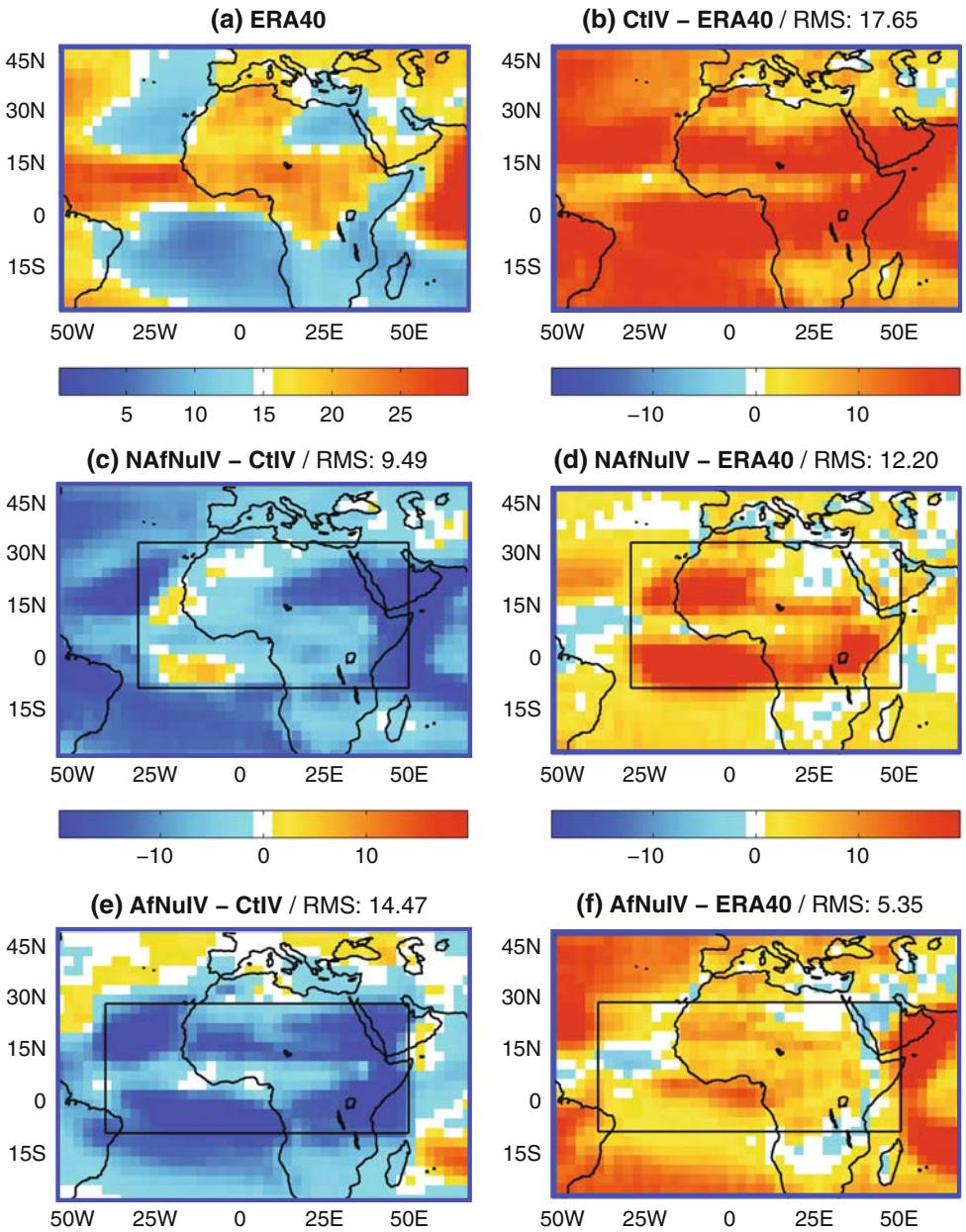

Fig. 6 Standard deviation of the unfiltered daily OLR field, which is then averaged in each grid point over the 1971–2000 period. In panel **c** to **f**, the domain of nudging is represented by a *black box*. The RMS value is calculated for all grid points inside the free (nudged) domain of NAfNuIV (AfNuIV) experiment, respectively (see Fig. 1)

resisting to the nudging and clearly reminiscent of the biases of CtIV experiment.

These results suggest a moderate improvement in the simulation of African intraseasonal variability. The African easterly wave patterns are nonetheless expected to be more realistic in the nudged experiments, including NAfNu (Fig. 7). Their propagation speed and location over Africa needs to be further examined, which will be the topic of a forthcoming study.

4.2 Weather regimes over North Atlantic and Europe

So far the focus has been on intraseasonal variability over the WAM region. In order to identify the possible link at intraseasonal timescale between the WAM circulation and the North Atlantic/European region, this section documents the impact of WAM circulation on weather regimes over Europe. Although daily geopotential height (Z500) has a deficit in variance in both simulations with and without AfNu over Europe of about 40% (not shown), stationary waves are sensitive to the nudging inside the WAM region which could impact the weather regimes over North Atlantic.

In this section, we used a cluster analysis based on the *k*-means partitioning algorithm (Michelangeli et al. 1995). It is applied to Z500 daily anomalies derived from the combined CtCl, CtIV, AfNuCl and AfNuIV simulations. ERA40 data were treated separately and the longest

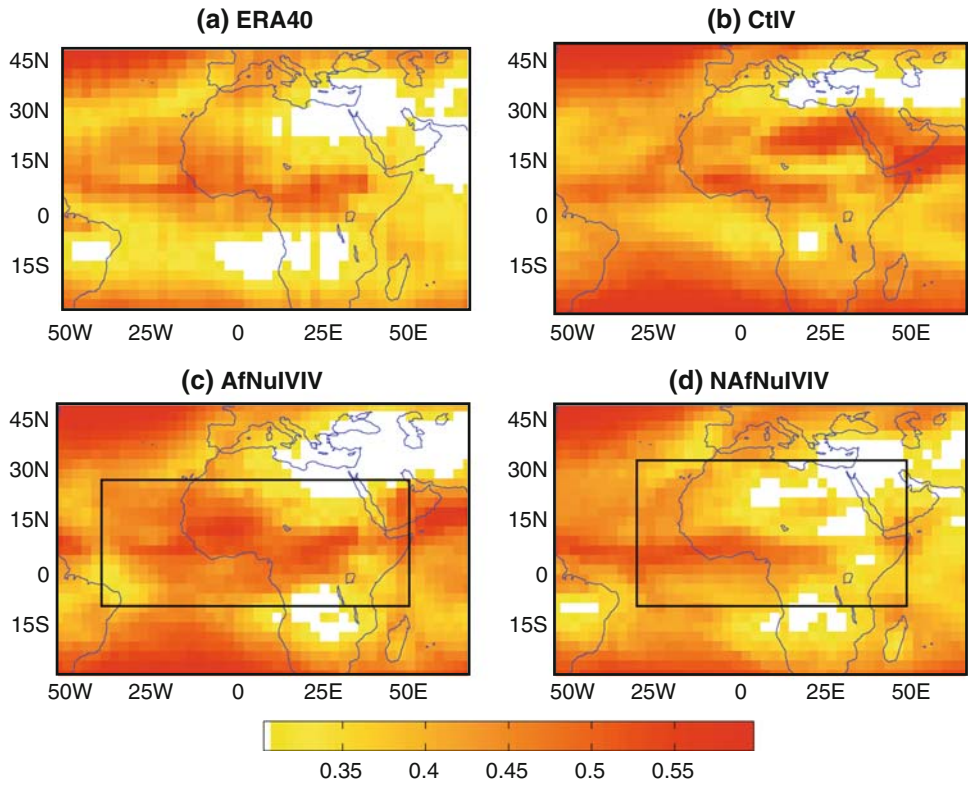

Fig. 7 Ratio between the standard deviation of the unfiltered daily OLR field and the 2–6-day bandpass filtered OLR for each grid point. The domain of nudging is represented by a *black box*

available period were used (1958–2001). We have verified that the weather regime patterns obtained for ERA40 are not changed by using only the 1971–2000 period. Daily summer maps (from June to September) are used and the analysis is performed over the North Atlantic-European region (20°N–80°N, 80°W–30°E) from 1971 to 2000. As in Cassou et al. (2005), we use $k = 4$ summertime regimes. Only regimes lasting at least 3 days and having a spatial correlation with the centroid greater than 0.25 are retained. With these two criteria, about 20% of the days are not classified and fall in the "other" category.

The centroids obtained from Arpege-Climat with or without nudging for the summer season and those obtained from the ERA40 reanalyses over the period 1958–2001 (Fig. 8) are very close to those derived by Cassou et al. (2005), namely the positive and negative phase of the summer North Atlantic Oscillation, respectively Blocking (BL) and NAO-, the Atlantic Low (AL) and the Atlantic Ridge (AR) regimes. Spatial correlations between the simulated and ERA40 centroids are all above 0.79. The AR regime shows the weakest correlation, due to the Arpege-Climat model difficulty in simulating the zonal character of this pattern. Overall, the model is able to reproduce relatively well the patterns of the four weather regimes (with or without nudging) over Europe for the summer season compared to the ERA40 data, despite a slight underestimation of intensity and a tendency to somewhat shift the maxima of the centroids to the West. The deficit of intensity is consistent with the lack of variance of the daily Z500 in the Arpege-Climat model and is partly related to the limited horizontal resolution of the model. Nevertheless, Arpege-Climat shows on the contrary too much variance in the tropics, thereby suggesting that the resolution is not the main explanation and that there could be also a lack of meridional export of the tropical variability. Note also that the Z500 variance maximum over the Atlantic is shifted westward in Arpege-Climat compared to ERA40, in line with the bias found in the day-to-day variability (not shown). Nudging over Africa does not remove this bias, although the Z500 variance is stronger over Northern Europe and weaker over the Mediterranean Sea.

Compared to ERA40, the seasonal mean occurrence of the regimes is relatively realistic in the control experiments with both climatological (CtCl) and observed (CtIV) monthly SSTs, except for the AL and BL regimes that are respectively overestimated by almost 50% and underestimated by about 25% (Fig. 9). Both regimes are very sensitive to the African nudging, which significantly modifies their frequency but with respectively a too strong decrease and a too strong increase compared to ERA40. Note also that the AfNu tends to favor the occurrence of the negative phase of the NAO regime, but this effect is

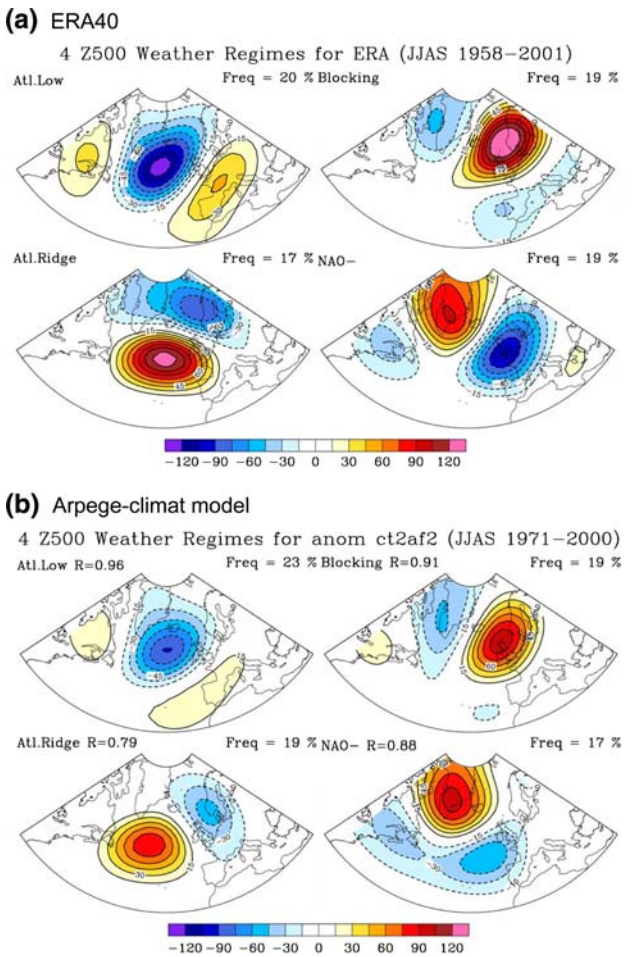

Fig. 8 JJAS Z500 (m) weather regimes computed over the North Atlantic/Europe sector from **a** ERA40 (*top four panels*) for the period 1958–2001. and **b** the four Arpege-Climat 30-years simulations with and without nudging over Africa (*bottom four panels*) for the period 1971–2000. R is the correlation coefficient with the centroid obtained from ERA40 and shown in *top four panels.* In each four panels, the *upper left panel* is the Atlantic Low regime having a JJAS frequency of occurrence of 20% for ERA40 and 23% for Arpege-Climat model respectively; the *upper right panel* is the Blocking regime having a JJAS frequency of occurrence of 19% for both ERA40 and Arpege-Climat model; the *lower right panel* is the Atlantic Ridge regime having a JJAS frequency of occurrence of 17% for ERA40 and 19% for Arpege-Climat model respectively; *the upper right panel* is the NAO-regime having a JJAS frequency of occurrence of 19% for ERA40 and 17% for Arpege-Climat model respectively

not necessarily significant given the stronger internal variability of this particular regime, as suggested by the difference between CtCl and CtIV (and also by the comparison with other ensembles driven by climatological SSTs). Note finally that the number of unclassified days (category "other" in Fig. 9) is larger in the ERA40 data compare to Arpege-Climat simulations, mostly because the model tends to produce fewer situations where regimes are lasting 2 days or less.

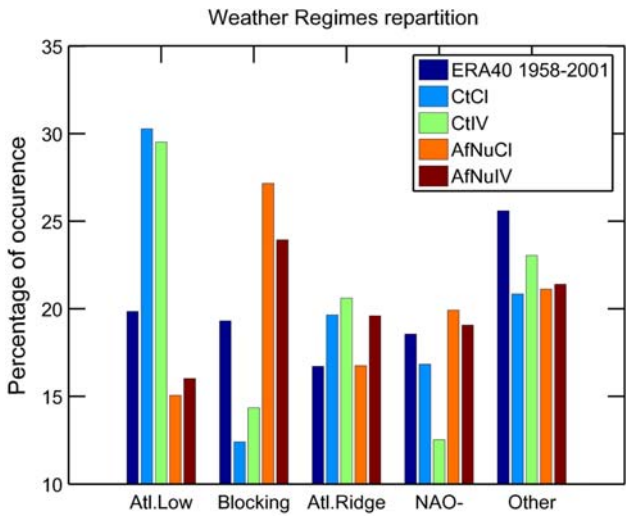

Fig. 9 JJAS weather regime frequency of occurrence (%) as obtained from ERA40 data and from the Arpege-Climat simulations with and without nudging. The category "other" contains days when a regime is lasting less than three consecutive days and/or with a correlation coefficient with the centroid smaller than 0.25

5 Interannual variability

5.1 West African variability

The reproducibility of the interannual WAM variability is explored in this section by computing the anomalies of two circulation and two rainfall indices: the West African Monsoon Index (WAMI, Fontaine et al. 1995, consisting in the difference between the 850 and 200 hPa zonal wind averaged over the domain [3°N–13°N, 20°W–20°E]), an AEJ index (reflecting the latitudinal location rather than the magnitude of the AEJ, Garric et al. 2002), a Sudan–Sahel and a Guinean coast rainfall index computed over [10°N–20°N;20°W–40°E] and [4°N–10°N;15°W–10°E] respectively. All seasonal anomalies are averaged over the JJAS period after a linear fit over the 1971–2000 period in order to get rid of the multi-decadal variability. Figure 10 compares the simulated anomalies against ERA40 and GPCC for the circulation and rainfall indices respectively. The interannual variability of all indices but the Guinean coast rainfall is poorly simulated in CtIV (no nudging, observed SSTs) with correlations lesser than 0.42. With the AfNu, not surprisingly, the correlation is almost 1 for the WAMI and AEJ indices (Fig. 10a, b). However, the amplitude of the AEJ variability is too weak compared to ERA40, in line with the southward shift of the AEJ climatology found in Fig. 2. For the Sudan–Sahel rainfall (Fig. 10c), the variability is largely improved by the AfNu, with a correlation coefficient going from 0.4 (in CtIV) to more than 0.7 (in AfNu), but again the amplitude is too low. The

improvement is not clear for the Guinean coast rainfall (Fig. 10d), which is mainly sensitive to the prescribed SST forcing.

More interestingly, the quasi-global nudging (NAfNu) leads to an improved simulation of the regional circulation variability (Fig. 10a, b); thereby suggesting that this experiment design is suitable to explore case studies. Nevertheless, the interannual variability of the precipitation indices is not clearly improved. This result is consistent with the limited improvement found in the rainfall climatology and emphasizes the limited sensitivity of the model deep convection to the large-scale forcing. Finally, the low correlation for the Guinean coast rainfall in NAfNuCl (with climatological SSTs) suggests again that rainfall over this region is mainly responding to the SST variability that modulates surface evaporation and thereby the advection of moisture from the ocean to the nearby continent.

To further highlight this effect, composites based on the seasonal mean SST averaged over the Gulf of Guinea [5°N–5°S; 30°W–10°E] for the JJAS 1971–2000 period were calculated. The ten warmest and the ten coldest years were extracted and a composite analysis of the 925 hPa horizontal wind and of precipitation was performed (Fig. 11). The ERA40 and GPCC composites confirm the hypothesis of a low-level convergence associated with more precipitation over the Guinean Coast, in agreement with the results of Fontaine and Janicot (1996). A weaker than normal monsoon flow prevails over West Africa in ERA40 associated with an increase of precipitation (Fig. 11a). The control simulation shows a decrease of the monsoon flow but fails however in simulating the coastal precipitation increase. Importantly, lower-layer wind convergence over Africa is better simulated in NAfNuIV experiment (Fig. 11d), concomitantly with the reduced trade winds over the western Atlantic that already prevailed in the ERA40 fields. The difference of daily precipitation between warm and cold years is significant over the Gulf of Guinea and the seashore of West and Central Africa only when observed SST are used (Fig. 11c, d). Because of the

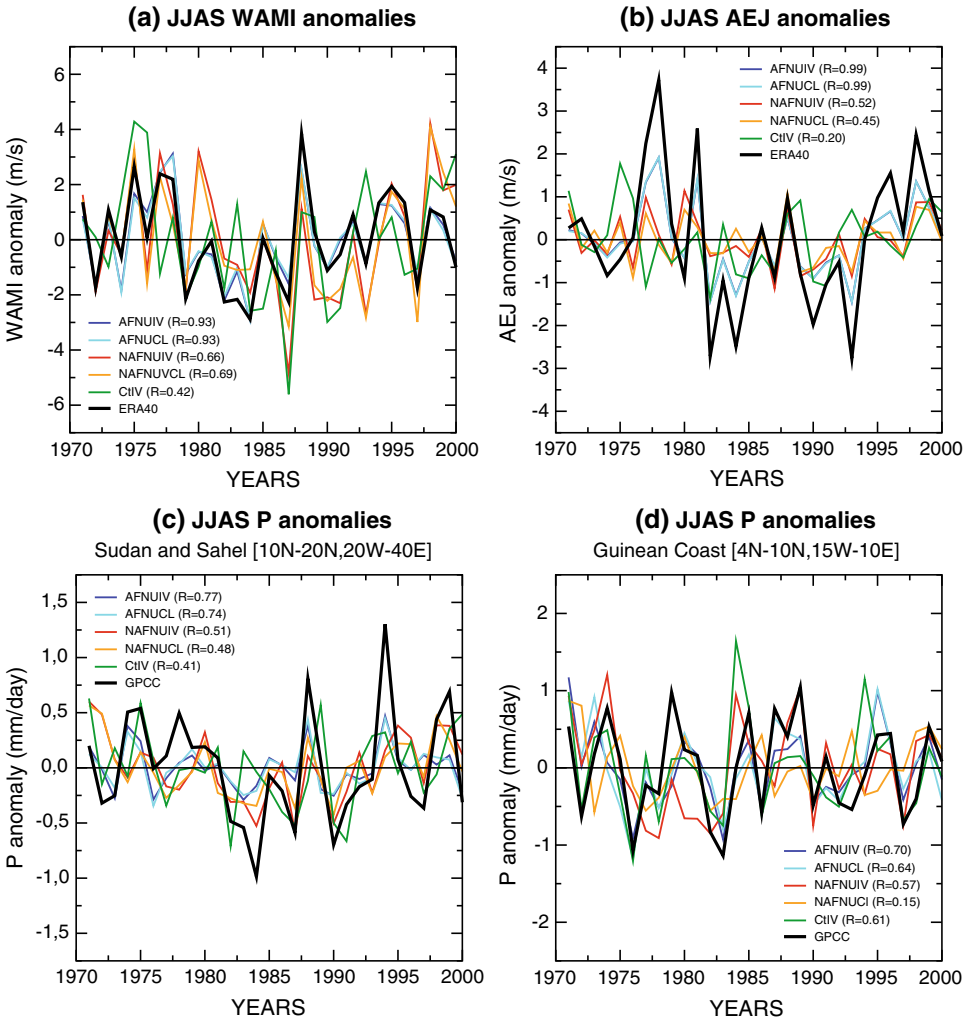

Fig. 10 Interannual variability of the anomalies of **a** WAMI index, **b** AEJ index, **c** Sudan–Sahel rainfall index and **d** Guinean coast rainfall index for ERA40 (**a**, **b**) and GPCP (**c**, **d**) respectively, and all the simulations. R denotes the correlation with ERA40 (**a**, **b**) and GPCP (**c**, **d**) respectively. All timeseries have been first detrended using a simple linear fit over the 1971–2000 period

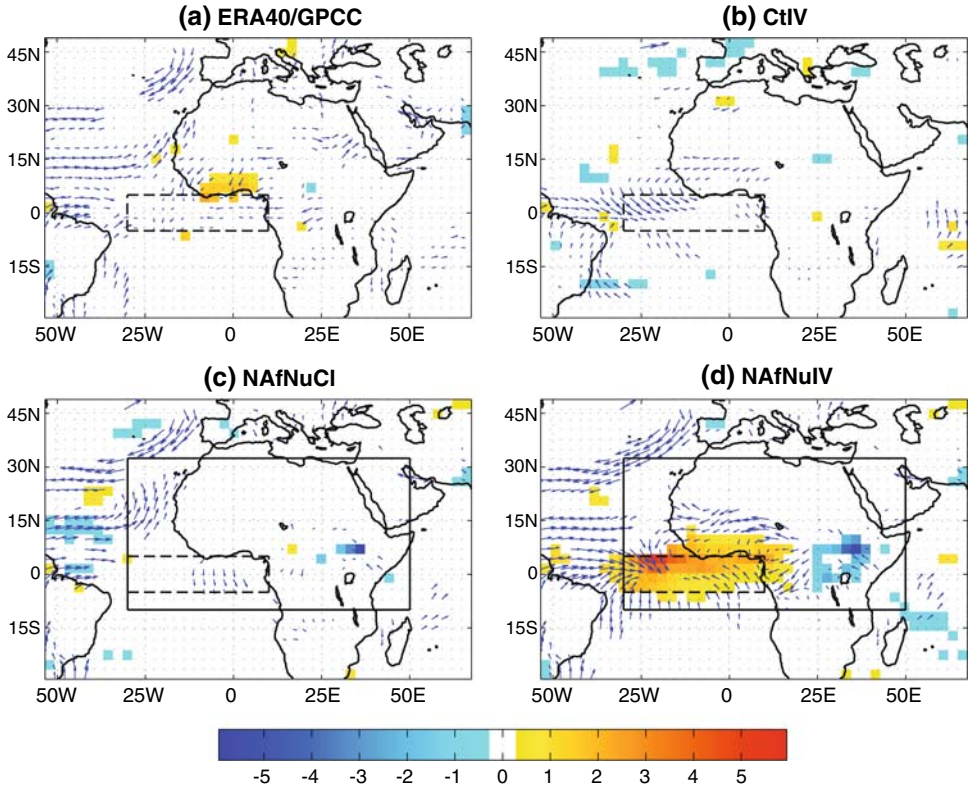

Fig. 11 Composites of wind at 925 hPa (*vectors*) and precipitation (*color shading*) over the 10 warmest SST years–10 coldest SST years over the Gulf of Guinea (*small black box*). The *large black box* shows the domain outside which nudging is applied. Only the precipitation (wind) differences that are significant at the 95% confidence level according to a two-tailed Student (Hotelling) test are shown

southern location of the simulated ITCZ and precipitation (Fig. 3) and also due to the weakening of the monsoon flow during warm years, these wet anomalies do not reach the hinterland parts of West Africa. Drier than normal conditions are on the opposite observed over the East African Highlands, a region experiencing its long dry period during this season of the year but concerned by important wet biases in Arpege-Climat model (see Fig. 3). The drier conditions found in the eastern part of Africa (Fig. 11d) might be partly due to the lack of feedback on the large-scale (outside of the free domain) moisture transport. In order to maintain a balance between moisture convergence and precipitation minus evaporation, the increase in precipitation over West Africa must be associated with a decrease in rainfall, which is here found over eastern Africa but has no counterpart in the observed composite.

Finally, the precipitation and wind anomalies are not significant in NAfNuCl, thereby confirming the dominant influence of the regional SST forcing on rainfall simulated interannual variability. WAM dynamics, AEJ location and Sahelian rainfall are nonetheless very weakly affected by Guinean SST (Fig. 10).

5.2 Tropical and extratropical variability

To explore the possible relationship between tropical and extratropical circulation, point-wise correlation maps with the Southern Oscillation Index (SOI, standardized pressure difference between Tahiti and Darwin) have been computed over the 1971–2000 period for the meridional wind at 200 hPa (Fig. 12) and precipitation (Fig. 13). The ERA40 200 hPa wind shows a weak ENSO teleconnection over the Gulf of Guinea and along the coast with negative correlations (Fig. 12a). The control simulation is not able to reproduce this connection (Fig. 12b). Moreover CtlV shows a teleconnection (with strong negative correlations) in a zonal band around 10°N over the African continent that is not realistic. In AfNu experiments, the connection over the Gulf of Guinea is weakly reproduced and the unrealistic connection along 10°N is reduced a lot.

The ERA40 upper-level winds show also a weak ENSO teleconnection over Europe, with positive correlations in the east which extent over central Africa and weak negative correlations in the west. The control simulation does not reproduce this dipole, but shows a strong wave-train pattern suggesting a Rossby-wave response to the summer ENSO forcing. In contrast, the teleconnection is more realistic though too strong in AfNuIV. While such a result would deserve a detailed analysis that is beyond the scope of the present study, it could be related to the improved simulation of the stationary waves found in AfNu over Europe (Fig. 5). This improvement is also found in the SOI correlations with JJAS precipitation anomalies (Fig. 13), which again highlight the spurious ENSO teleconnection

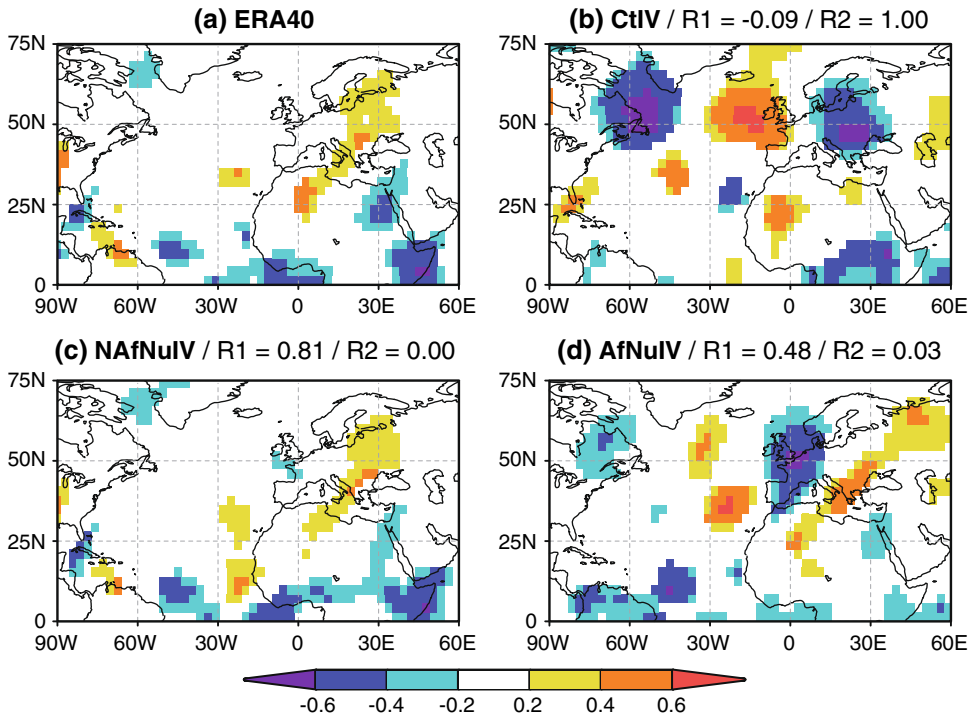

Fig. 12 Point-wise correlations between SOI index and JJAS 200-hPa meridional wind. R1 denotes the correlation with ERA40 (panel **a**) and R2 the correlation with CtIV (panel **b**). In panels **c** and **d**, the domain of nudging is represented by the *black box*. Only correlations being significant at the 90% confidence level according to a phase-scrambled bootstrap test are shown

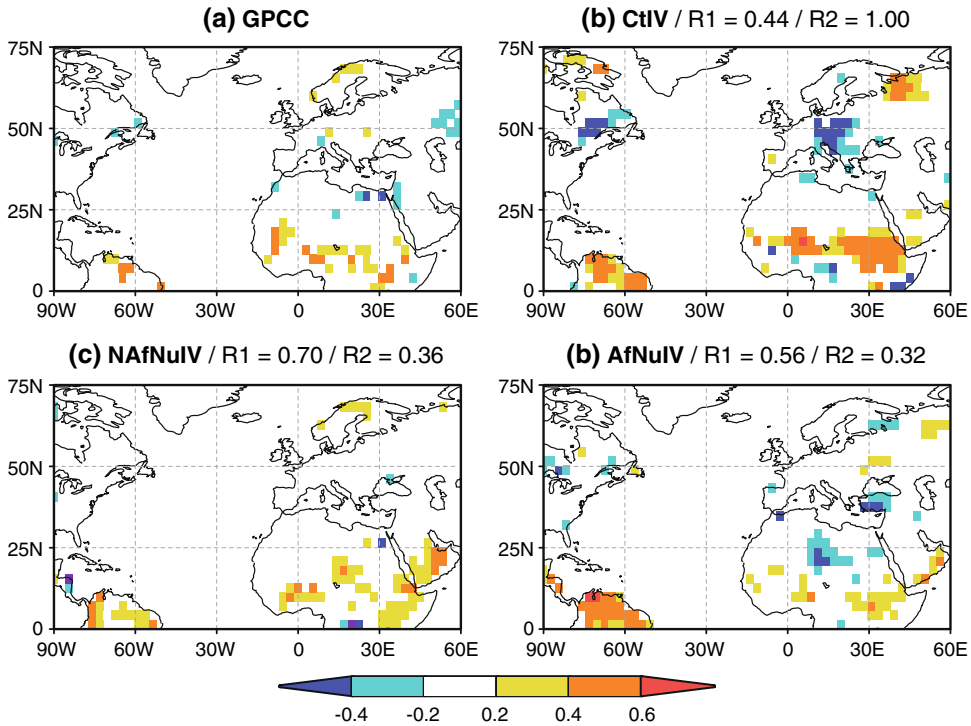

Fig. 13 Same as Fig. 12 but for point-wise correlations between SOI index and JJAS precipitation. R1 is the correlation with GPCC and R2 the correlation with CtIV. Only correlations being significant at the 90% confidence level according to a phase-scrambled bootstrap test are shown

found in CtIV. Interestingly, the positive correlations between SOI and precipitation between 10°N and 20°N over Africa are amplified by the control simulation (Fig. 13). Both nudged experiments captured better this weak teleconnection. Note finally that the well-known ENSO teleconnection with the WAM rainfall (Fontaine and Janicot 1996; Joly et al. 2007) is only marginally improved in NAfNuIV compared to CtIV, which simply suggests that this remote impact is reasonably captured by the model when observed SSTs are prescribed.

6 Summary, conclusions and prospects

Coupled ocean–atmosphere general circulation models are now widely used to produce both seasonal forecasts and climate scenarios, but our understanding of natural climate variability has long been based on atmospheric simulations driven by SST, in which the atmosphere is supposed to adjust to the oceanic variability. Here we propose a new and complementary perspective by using guided atmospheric experiments, i.e. simulations in which the atmosphere is nudged regionally toward the ERA40 reanalyses. The aim is to explore to what extent a "perfect" simulation of the WAM would improve the simulation of the global atmospheric circulation, and conversely, to what extent a "perfect" simulation outside of the WAM domain would improve the simulation of the monsoon. The impact of the nudging has been studied on mean climate as well as on both intraseasonal and interannual timescales. Results suggest that the Arpege-Climat model responds physically to the strong relaxation, and does not trigger spurious features at the boundary of the nudging domain. Note however that the nudging does not lead to a systematic reduction of the model biases. This result does not mean that the nudging is not a powerful tool to diagnose the model errors, but suggests that errors have different origins and that correcting some of them is not necessarily sufficient to improve the simulation outside of the nudging domain.

Without nudging, the Arpege-Climat model is able to capture the three dominant features of the atmospheric circulation over West Africa (namely the lower-layer monsoon flow, the mid-tropospheric African Easterly Jet and the upper-layer Tropical Easterly Jet), but with marked biases. As far as the quasi-global (NAfNu) nudging is concerned, the main conclusion is the limited improvement not only of the mean summer monsoon rainfall climatology over West Africa but also of the 3D monsoon dynamics, thereby showing that model biases mainly originate from regional processes rather than remote effects. The same conclusion applies to intraseasonal variability, though a more detailed study would be necessary to distinguish between the various modes that have been documented over West Africa. Conversely, the quasi-global nudging allows a significant improvement of the interannual variability, at least for the large-scale circulation indices, and suggests that the nudging technique provides an interesting framework to design case studies and explore the relevance of regional versus remote factors in monsoon variability.

Moving to the African (AfNu) nudging experiments, no dramatic change was found on the model climatology outside the nudging region. Nevertheless, an impact was found on the simulation of the extratropical stationary waves. The impact is positive in the winter hemisphere (not shown), but does not clearly leads to an improved climatology in the summer (i.e. northern) hemisphere. This is particularly true over the North Atlantic sector where some features of the summer climatology (the stationary wave patterns and the frequency of occurrence of some weather regimes) are "overcorrected" in AfNu compared to the control experiment (i.e. the nudging leads to opposite biases and sometimes a stronger RMS). At interannual timescale, on the one hand, the Sudan–Sahel rainfall variability is largely improved by the AfNu even if the amplitude remains too low. On the other hand, the AfNu seems to improve the simulation of the tropical–extratropical teleconnections. Indeed, the spurious ENSO teleconnection found over Europe in the control experiment is significantly improved in AfNu. This interesting result would however deserve further investigation and is not easy to interpret given the mixed impact of the nudging on the European stationary wave and weather regime climatology.

Note that additional sensitivity tests have been conducted where only dynamical prognostic variables have been relaxed (u, v) or where the relaxation strength has been reduced (not shown) without dramatic change in the results, but a weaker magnitude in the model response in the latter experiments. In the near future, further experiments will be devoted to case studies where ensembles will be conducted for a specific summer season and will be compared to AfNu or NAfNu in order to isolate the nudging contribution to interannual variability. Moreover, other tropical nudging domains will be tested in the framework of the IRCAAM project (South Asia, Central America as well as the entire tropical belt) in order to further explore the tropical–extratropical teleconnections related to the monsoon climates, but also the possible connections between the Indian and African monsoons. Finally, the relevance of land surface and SST feedbacks in such teleconnections will be investigated in additional sensitivity experiments where a soil moisture nudging and/or a coupling with a mixed ocean layer will be also implemented.

Acknowledgments This study has been mainly supported by the French National Research Agency in the framework of the IRCAAM (Influence Réciproque des Climats d'Afrique de l'ouest, du sud de l'Asie et du bassin Méditerranéen, http://www.cnrm.meteo.fr/ircaam/) project. Thanks are also due to the AMMA (African Monsoon Multidisciplinary analysis, http://www.amma-international.org) project funded by the European commission sixth framework program. The authors are very grateful to Michel Déqué, Virginie Lorant and Christophe Cassou for their support in using the Arpege-Climat model and the tools for weather regime analysis. The authors are also grateful to the two reviewers for their thoughtful and constructive reviews, which helped improving the manuscript.

References

Bougeault P (1985) A simple parametrization of the large-scale effects of cumulus convection. Mon Weather Rev 113:2108–2121. doi:10.1175/1520-0493(1985)113<2108:ASPOTL>2.0.CO;2

Cassou C, Terray L, Phillips AS (2005) Tropical Atlantic influence on European heat waves. J Clim 18:2805–2811. doi:10.1175/JCLI3506.1

Cook KH, Vizy EK (2006) Coupled model simulations of the West African monsoon system: twentieth and twenty-first-century simulations. J Clim 19:3681–3703. doi:10.1175/JCLI3814.1

Douville H, Salas-Mélia D, Tyteca S (2006) On the tropical origin of uncertainties in the global land precipitation response to global warming. Clim Dyn 26:367–385. doi:10.1007/s00282-005-0088-2

Fontaine B, Janicot S (1996) Seas surface temperature fields associated with West African rainfall anomaly types. J Clim 9:2935–2940. doi:10.1175/1520-0442(1996)009<2935:SSTFAW>2.0.CO;2

Fontaine B, Janicot S, Moron V (1995) Rainfall anomaly patterns and wind field signals over West Africa in August (1958–1989). J Clim 8:1503–1510. doi:10.1175/1520-0442(1995)008<1503:RAPAWF>2.0.CO;2

Garric G, Douville H, Déqué M (2002) Prospects for improved seasonal predictions of monsoon precipitation over Sahel. Int J Climatol 22(3):331–345. doi:10.1002/joc.736

Hoskins BJ, Ambrizzi T (1993) Rossby wave propagation on a realistic longitudinal varying flow. J Atmos Sci 50:1661–1671. doi:10.1175/1520-0469(1993)050<1661:RWPOAR>2.0.CO;2

Janicot S, Trzaska S, Poccard I (2001) Summer Sahel-ENSO teleconnection and decadal time scale SST variations. Clim Dyn 18:303–320. doi:10.1007/s003820100172

Janicot S, Mounier F, Hall NMJ, Leroux S, Sultan B, Kiladis GN (2009) The dynamics of the West African monsoon. Part IV: Analysis of the 25–90-day variability of convection and the role of the Indian monsoon. J Clim 22:1541–1565

Joly M, Voldoire A, Douville H, Terray P, Royer J-F (2007) African monsoon teleconnections with tropical SSTs: validation and evolution in a set of IPCC4 simulations. Clim Dyn 29:1–20. doi:10.1007/s00382-006-0215-8

Jung T, Palmer T, Rodwell M, Serrar S (2008) Diagnosing forecast error using relaxation experiments. ECMWF Newsletter No. 116:24:34, Summer 2008

Matthews AJ (2004) Intraseasonal variability over tropical Africa during northern summer. J Clim 17:2427–2440. doi:10.1175/1520-0442(2004)017<2427:IVOTAD>2.0.CO;2

Michelangeli P-A, Vautard R, Legras B (1995) Weather regimes: recurrence and quasi stationarity. J Atmos Sci 52:1237–1256. doi:10.1175/1520-0469(1995)052<1237:WRRAQS>2.0.CO;2

Mohino Harris E, Rodríguez-Fonseca B, Gervois S, Janicot S, Losada Doval T, Bader J, Ruti PM, Chauvin F (2008) SST-forced signals on West African rainfall from AGCM simulations—Part I: Intercomparison of models. Clim Dyn (submitted)

Moron V, Philippon N, Fontaine B (2004) Simulation of West African monsoon circulation in four atmospheric general circulation models forced by prescribed sea surface temperature. J Geophys Res 109:D24105. doi:10.1029/2004JD004760

Pohl B, Janicot S, Fontaine B, Marteau R (2009) Implication of the Madden–Julian Oscillation in the 40-day variability of the West African Monsoon. J Clim 22:3769–3785

Raicich F, Pinardi N, Navarra A (2003) Teleconnections between Indian monsoon and Sahel rainfall and the Mediterranean. Int J Clim 23:173–186. doi:10.1002/joc.862

Redelsperger J-L, Thorncroft CD, Diedhiou A, Lebel T, Parker DJ, Polcher J (2006) African Monsoon multidisciplinary analysis. An international research project and field campaign. Bull Am Meteorol Soc 87:1739–1746. doi:10.1175/BAMS-87-12-1739

Rodwell MJ, Hoskins BJ (1996) Monsoons and the dynamics of deserts. QJR Meteorol Soc 122:1385–1404. doi:10.1002/qj.49712253408

Rowell DP (2001) Teleconnections between the tropical Pacific and the Sahel. QJR Meteorol Soc 127:1683–1706. doi:10.1002/qj.49712757512

Ruti PM, Dell' Aquila A (2008) The 20th century AEJ and AEWs in reanalyses and IPCC simulations. AMMA report

Salas y Mélia D, Chauvin F, Déqué M, Douville H, Guérémy JF, Marquet P, Planton S, Royer J-F, Tyteca S (2005) Description and validation of CNRM-CM3 global coupled climate model, Note de Centre du GMGEC No. 103, Décembre 2005

Sperber KR, Palmer TN (1996) Interannual tropical rainfall variability in general circulation model simulations associated with the Atmospheric Model Intercomparison Project. J Clim 9:2727–2750. doi:10.1175/1520-0442(1996)009<2727:ITRVIG>2.0.CO;2

Sultan B, Janicot S, Diedhiou A (2003) The West African monsoon dynamics. Part I: Documentation of intraseasonal variability. J Clim 16:3389–3406. doi:10.1175/1520-0442(2003)016<3389:TWAMDP>2.0.CO;2

Uppala SM, Kallberg PW, Simmons AJ et al (2005) The ERA-40 reanalysis. QJR Meteorol Soc 131:2961–3012. doi:10.1256/qj.04.176

Von Storch H, Langenberg H, Feser F (2000) A spectral nudging technique for dynamical downscaling purposes. Mon Weather Rev 128:3664–3673. doi:10.1175/1520-0493(2000)128<3664:ASNTFD>2.0.CO;2

Webster PJ, Magana VO, Palmer TN, Shukla J, Tomas RA, Yanai M, Yasunari T (1998) Monsoons: processes, predictability, and the prospects for prediction. J Geophys Res 103:14451–14510. doi:10.1029/97JC02719